29th Congress of the International Council of the Aeronautical Sciences
St. Petersburg, Russia; September 7-12, 2014

A NON-COOPERATIVE BI-LEVEL OPTIMAL CONTROL PROBLEM FORMULATION FOR NOISE MINIMAL DEPARTURE TRAJECTORIES

M. Richter*, M. Bittner*, M. Rieck* , F. Holzapfel*
***Institute of Flight System Dynamics, Technische Universität München**

Keywords: *trajectory optimization, aircraft noise, aircraft procedures*

Abstract

A bi-level optimal control problem formulation is presented that allows the determination of noise minimal departure trajectories. It consists of an upper level optimization problem and multiple embedded lower level optimal control problems. The upper level problem is concerned with determining the set of RNAV (RNP) waypoints minimizing the noise impact on the population. It is called non-cooperative as unlike in previous studies the embedded lower level problems do not minimize noise impact but direct operational costs.

1 Introduction

Air traffic has been growing continuously over the last decades with revenue passenger kilometers doubling nearly every fifteen years and this trend is expected to last in the future. Today, major airports are facing more than a thousand aircraft movements a day leading to considerable annoyance of surrounding communities in terms of emissions and noise. Hence, plans for new airports as well as extensions of existing ones are strongly opposed by local population. Due to the rise of satellite based navigation systems and the upcoming availability of GBAS/SBAS systems it nowadays becomes possible to define curved trajectories instead of the conventional straight flight tracks restricted by the use of ILS and VOR/NDB navaids. To ensure continuous air traffic growth that is well accepted by the population considerable research has been dedicated to the design of take-off and approach procedures minimizing the environmental impact of aviation. Often, an optimal control problem is formulated and solved by direct methods [1, 2, 3]. Recently, we extended this approach by using a bi-level optimal control problem formulation leading to more realistic trajectories and allowing the computation of robust noise minimal trajectories [4]. However, in previous research it was assumed that the (lower) optimal control problems minimize the noise impact. From a practical point of view this is unlikely as airlines tend to minimize their direct operational costs and not noise impact. Hence, in this paper we introduce a non-cooperative bi-level approach where the upper level problem tries to minimize the noise impact but the lower level problems try to minimize their direct operational cost measured by a weighted combination of flight time and fuel burned.

2 Bi-level Optimal Control

The problem is formulated as a bi-level optimal control problem [5] comprising an upper level optimization problem and one or multiple embedded optimal control problems. Within this kind of problems, the cost and constraint functions of the upper level depend on the (optimal)

solution of the lower levels, which in turn depend on the parameter vector $\boldsymbol{p}$ of the upper level. In a mathematical form, the bi-level optimal control problem can be formulated as follows:

$$\begin{aligned} \underset{p\in P}{\text{minimize}} \quad & J_u(\boldsymbol{x}_i^*(t),\boldsymbol{u}_i^*(t),t_i^*,\boldsymbol{p}) \\ \text{subject to} \quad & \boldsymbol{G}_u(\boldsymbol{x}_i^*(t),\boldsymbol{u}_i^*(t),t^*,\boldsymbol{p}) \leq \boldsymbol{0} \end{aligned} \tag{1}$$

where $\boldsymbol{x}_i^*$, $\boldsymbol{u}_i^*$ and t_i^* are the solution of the $i^{th}, i = 1,...,n$, optimal control problem:

$$\begin{aligned} \underset{\boldsymbol{x},\boldsymbol{u},t}{\text{minimize}} \quad & J_l = \Phi(\boldsymbol{x}(t_f),t_f,\boldsymbol{p}) \\ & \quad + \int_{t_0}^{t_f} g(\boldsymbol{x}(t),\boldsymbol{u}(t),t,\boldsymbol{p})dt \\ \text{subject to} \quad & \dot{\boldsymbol{x}}(t) = \boldsymbol{f}(\boldsymbol{x}(t),\boldsymbol{u}(t),t,\boldsymbol{p}) \\ & \boldsymbol{0} \geq \boldsymbol{G}_l(\boldsymbol{x}(t),\boldsymbol{u}(t),t,\boldsymbol{p}) \end{aligned} \tag{2}$$

To solve the bi-level optimal control problem the lower level optimal control problems are transcribed using the Hermite-Simpson-Collocation Method [6] to a Nonlinear-Programming Problem (NLP). The NLPs as well as the upper level problem can then be solved using well-known parameter optimization algorithms, such as SNOPT [14], IPOPT [9] or WORHP [13]. However, these algorithms require the gradient of the cost and constraint functions with respect to the optimization parameters. While this can be done quite easily for the lower level problem using numerical differentiation methods or an automatic differentiation package like ADOLC , this is more evolved for the upper level problem. Computing the jacobian of the upper level problem using finite differences would require at least one additional solution of all lower level optimal control problems for each parameter in the upper level parameter vector $\boldsymbol{p}$ leading to significant increase in computational effort. However, if the jacobian of the upper level objective function vector $\boldsymbol{F}_u$ (comprising cost and constraint functions), which depends on K lower level problems, is written as:

$$\nabla_{\boldsymbol{p}}\boldsymbol{F}_u(\boldsymbol{p},\boldsymbol{z_1},\boldsymbol{z_2},...\boldsymbol{z_K}) = \frac{\partial \boldsymbol{F}_u}{\partial \boldsymbol{p}} + \sum_{j=1}^{K} \frac{\partial \boldsymbol{F}_u}{\partial \boldsymbol{z}_j} \cdot \frac{d\boldsymbol{z}_j}{d\boldsymbol{p}}, \tag{3}$$

it becomes clear that it can be computed efficiently using the post-optimal sensitivity analysis for each lower level problem. This method allows the calculation of the sensitivity matrix $d\boldsymbol{z}/d\boldsymbol{p}^T$, which gives the change of the optimization parameters $\boldsymbol{z} = (\boldsymbol{x},\boldsymbol{u},t)$ of the discretized optimal control problem due to a change in the parameter vector $\boldsymbol{p}$. To compute the sensitivity matrix of one lower level optimal control problem the following relation is used [7].

$$\begin{pmatrix} \frac{d\boldsymbol{z}}{d\boldsymbol{p}} \\ \frac{d\boldsymbol{\lambda}}{d\boldsymbol{p}} \end{pmatrix} = \begin{pmatrix} \boldsymbol{L}_{0,\boldsymbol{zz}}(\boldsymbol{z},\boldsymbol{\lambda},\boldsymbol{p}) & \boldsymbol{G}_{\boldsymbol{z}}^{aT} \\ \boldsymbol{G}_{\boldsymbol{z}}^{a} & \boldsymbol{0} \end{pmatrix}^{-1} \begin{pmatrix} \boldsymbol{L}_{0,\boldsymbol{z},\boldsymbol{p}}(\boldsymbol{z},\boldsymbol{\lambda},\boldsymbol{p}) \\ \boldsymbol{G}_{\boldsymbol{p}}^{a}(\boldsymbol{z},\boldsymbol{p}) \end{pmatrix} \tag{4}$$

In Eq. (4) $\boldsymbol{G}_l^a$ is the set of active constraint functions of the discretized optimal control problem and $\boldsymbol{G}_{l,\boldsymbol{z}}^a$ and $\boldsymbol{G}_{l,\boldsymbol{p}}^a$ are the derivatives with respect to the optimization variables $\boldsymbol{z}$ and the parameters $\boldsymbol{p}$, respectively. The set of active constraints comprises the collocation defects resulting from the discretization of the model dynamics, all equality constraints and the inequality constraints that are at their upper bounds. For each lower level problem the Lagrangian function L_0 is defined as:

$$L_0(\boldsymbol{z},\boldsymbol{\lambda},\boldsymbol{p}) = J_l + \sum_{i=1}^{N} \lambda_i \cdot G_{l,i} \tag{5}$$

In here, J_l is the cost function of the discretized lower level optimal control problem and λ_i is the lagrange multiplier associated with $G_{l,i}$. Note, that lagrange multipliers for inactive constraints are equal to zero. $L_{0,\boldsymbol{zz}}$ and $L_{0,\boldsymbol{zp}}$ are the respective second derivatives of the Lagrangian.

3 Upper Level Optimization Problem

The upper level optimization problem is concerned with determining the position of a fixed set of RNAV (RNP) waypoints defining a departure procedure to minimize perceived noise on ground under the assumption that the departing aircraft perform cost optimal operations. In the following, the parameterization of the horizontal flight path, the noise cost function and additional constraints are introduced.

3.1 Flight Path Parameterization

For simplicity, it is assumed that the RNAV (RNP) trajectory consists only of Track-To-Fix (TF) and Radius-To-Fix (RF) segments as depicted in Fig. 1.

Given a reference velocity V_0, a nominal duration $\Delta\tau$ can be assigned to each segment. Furthermore, the nominal turn rate χ' can be computed from the radius R of a RF segment by:

$$\chi' = \frac{V_0}{R} \tag{6}$$

Thus, given the initial position (X_0, Y_0) and the initial course angle χ_0, the horizontal flight path consisting of N segments is completely defined by the following parameter vector:

$$\boldsymbol{p} = (X_0, Y_0, \chi_0, \Delta\tau_1, \chi'_1, ..., \Delta\tau_N, \chi'_N), \tag{7}$$

where the nominal turn rate χ' for a TF segment is of course zero.
The reference speed is taken from ICAO Doc 8168 [8], where maximum speeds for turning departures for different aircraft categories are listed.

3.2 Cost Function

To determine the noise impact of a departing aircraft on the local population the number of awakenings as defined by the Federal Interagency Committee on Aviation Noise (FICAN) [15] is used. The proposed relationship computes the percentage of persons likely to awake due to a noise event at a specific location as a function of the indoor Sound Exposure Level (SEL).

$$\%_{awak} = 0.0087 \cdot (SEL_{indoor} - 30dB)^{1.79}, \tag{8}$$

The percentage of awakenings is then multiplied with the number of persons allocated at the current receiver. Finally, the total number of awakenings is given as the sum over all receivers:

$$n_{awak} = \sum_{i=1}^{N} \%_{awak,i} \cdot P_i \tag{9}$$

The indoor SEL can be computed from the outdoor SEL by substracting 20.5dB representing the typical sound absorption of a house [1]. The SEL itself is given by the integration of the Sound Pressure Level L_A:

$$SEL = \int_{t_0}^{t_f} 10^{0.1 \cdot L_A(t)} dt \tag{10}$$

The history of the Sound Pressure Level L_A required by Eq. (10) is computed using the aircraft noise model developed by Figlar [12], which is based on ECAC Doc 29 and adapted for optimization purposes. It divides the flight path into infinitesimal segments such that sound pressure level L_A equals the maximum sound pressure level $L_{A,max}$ for that segment, i.e. $L_A(t) = L_{A,max}$, and approximates the noise-power-distance tables given e.g. in the FAA's Integrated Noise Model (INM) [10] by an analytic function of the form:

$$L_A = c_0 + c_1 \cdot T_{corr} + c_2 \cdot \lg d + c_3 \cdot (\lg d)^2, \tag{11}$$

where c_i are the coefficients of the fit, T_{corr} is the corrected net thrust of one engine and d is the distance between the receiver and the aircraft. Eq. (11) is corrected by the lateral attenuation factor Λ to yield the following equation

$$L_A = c_0 + c_1 \cdot T_{corr} + c_2 \cdot \lg d + c_3 \cdot (\lg d)^2 - \Lambda, \tag{12}$$

where the value of Λ depends on the elevation angle, i.e. the angle between the line of sight vector from receiver to aircraft and the horizontal plane, and the distance d. The noise model was validated against INM and close agreement was found. However, it must be noted that the original noise-power-distance tables are very limited and do not allow to model configuration changes. The position of the receivers are computed from a population database [11] using a k-means clustering algorithm. The cost function of the upper level problem can the be written as a weighted combination of mean flight time (resulting from the lower level problems) and the number of awakenings:

$$J_u = w_1 \cdot n_{awak} + w_2 \cdot \bar{t}_f \tag{13}$$

3.3 Constraints

To ensure that the aircraft can follow the prescribed horizontal track, it is necessary to limit

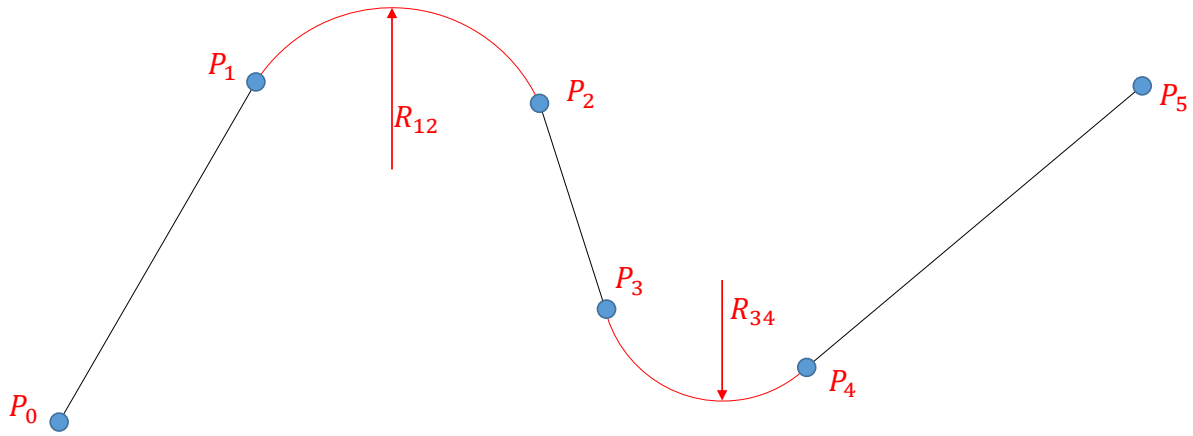

Fig. 1 Horizontal flight path

the nominal turn rate $\chi\prime$. To this end, a minimum/maximum bank angle of $\pm 20°$ is assumed and the resulting minimum/maximum turn rate is:

$$\chi\prime_{min/max} = \frac{g}{V_0} \cdot \tan \mu_{min/max} \tag{14}$$

4 Lower Level Optimal Control Problem

The lower level optimal control problem is concerned with finding the control and state histories that minimize the operational cost of the flight while following a prescribed horizontal path.

4.1 Cost Function

In here, the operational cost is modeled as a weighted sum of flight time and fuel consumption.

$$J_l = w \cdot t_f + (1-w) \cdot m_{fuel} \tag{15}$$

4.2 Simulation Model

To describe the dynamics of the aircraft a non-linear point mass model is used, which is described in this section. To simplify the calculations, a flat, non-rotating earth is assumed. Therefore, the position equations of motion with respect to a north-east-down frame O fixed at the runway threshold are given by Eq. (16).

$$\begin{pmatrix} \dot{x}^G \\ \dot{y}^G \\ \dot{z}^G \end{pmatrix}_K^O = \begin{pmatrix} V_K^G \cdot \cos\chi_K^G \cdot \cos\gamma_K^G \\ V_K^G \cdot \sin\chi_K^G \cdot \cos\gamma_K^G \\ -V_K^G \cdot \sin\gamma_K^G \end{pmatrix}_K^O, \tag{16}$$

where V_K^G is the absolute kinematic velocity of the aircraft and χ_K^G and γ_K^G are the kinematic course and flight path angle.

The translation equations of motion are written with respect to the flight path reference frame K. Following Newton's second law, they can be written as:

$$\begin{pmatrix} \dot{V}_K^G \\ \dot{\chi}_K^G \\ \dot{\gamma}_K^G \end{pmatrix}_K^{OO} = \frac{1}{m} \cdot \begin{pmatrix} (\sum F_{x,K}^G) \\ (\sum F_{y,K}^G)/(V_K^G \cdot \cos\gamma_K^G) \\ (\sum F_{z,K}^G)/V_K^G \end{pmatrix}, \tag{17}$$

where the sum of forces acting on the aircraft's center of gravity comprises aerodynamic and propulsion force as well as gravitational force, which is modeled as a constant force in z-direction of the NED-frame. The aerodynamic forces are computed in the aerodynamic frame A taking into account wind effects. The propulsion force is assumed to act in x-direction of the kinematic frame. Both aerodynamic and propulsion forces are modeled according to the Base Of Aircraft Data Family 4 (BADA4) published by EUROCONTROL. Furthermore, the fuel flow model of BADA4 is implemented as well.

Thus, the state of the aircraft is fully described by the following state vector:

$$\boldsymbol{x} = (x^G, y^G, z^G, V_K^G, \chi_K^G, \gamma_K^G, m)^T \tag{18}$$

and is influenced by the lift coefficient C_L,

the thrust lever position C_T and the aerodynamic bank angle μ_A:

$$\boldsymbol{u} = (C_L, C_T, \mu_A)^T \tag{19}$$

From an optimization point of view, it turned out to be beneficial to perform the integration in nominal time τ, where the relationship between real time t and nominal time τ is given by:

$$\dot{\tau} = \frac{x_T' \cdot \dot{x}^G + y_T' \cdot \dot{y}^G}{x_T'^2 + y_T'^2 + x_T'' \cdot (x_T - x^G) + y_T'' \cdot (y_T - y^G)}, \tag{20}$$

where x_T and y_T are the position along the track with minimum distance to the aircraft. The differential equations for the track are given by:

$$\begin{aligned} x_T' &= V_0 \cdot \cos\chi_T \\ y_T' &= V_0 \cdot \sin\chi_T \\ \chi_T' &= \chi_{T,CMD}' \end{aligned} \tag{21}$$

To integrate the aircraft state dynamics in nominal time, they are therefore multiplied with the inverse of $\dot{\tau}$:

$$\boldsymbol{x}' = \dot{\boldsymbol{x}} \cdot \frac{1}{\dot{\tau}} \tag{22}$$

The deviation of the aircraft from the prescribed track in x- and y-direction can then be propagated by the following differential equations:

$$\begin{aligned} \Delta x' &= x_T' - \dot{x}^G/\dot{\tau} \\ \Delta y' &= y_T' - \dot{y}^G/\dot{\tau} \end{aligned} \tag{23}$$

4.3 Path Constraints

By limiting Δx and Δy it is ensured that the aircraft follows the prescribed track:

$$\begin{aligned} -20m \leq &\Delta x \leq 20m \\ -20m \leq &\Delta y \leq 20m \end{aligned} \tag{24}$$

To generate realistic aircraft departure operations and to respect the limits of the aircraft model a set of constraints is introduced. First of all, the following bounds for the controls are given:

$$\begin{aligned} 0 \leq C_L &\leq C_{L,max} \\ 0 \leq C_T &\leq 1 \\ -20^\circ \leq \mu_A &\leq 20^\circ, \end{aligned} \tag{25}$$

where the upper limit for the lift coefficient can be deduced from BADA 4. Furthermore, the calibrated velocity, which is estimated by:

$$V_{CAS} = \sqrt{\frac{\rho}{\rho_0}}, \tag{26}$$

is limited as follows:

$$1.3 \cdot V_{stall} \leq V_{CAS} \leq 250kt, \tag{27}$$

where the stall speed depends on the current configuration of the aircraft.
Finally, two constraints concerning the calibrated airspeed and the altitude are introduced to generate realistic flight profiles. Both are enforced to increase monotonically during the departure:

$$\begin{aligned} \dot{V}_{CAS} &\geq 0 \\ \dot{h} &\geq 0 \end{aligned} \tag{28}$$

5 Numerical Example

In this section a numerical example is presented. Fig. 2 shows the population distribution together with an initial guess for the departure procedure. To compute the noise impact of a single flight onto the population, the population distribution around the airport is clustered into 10,000 receivers.

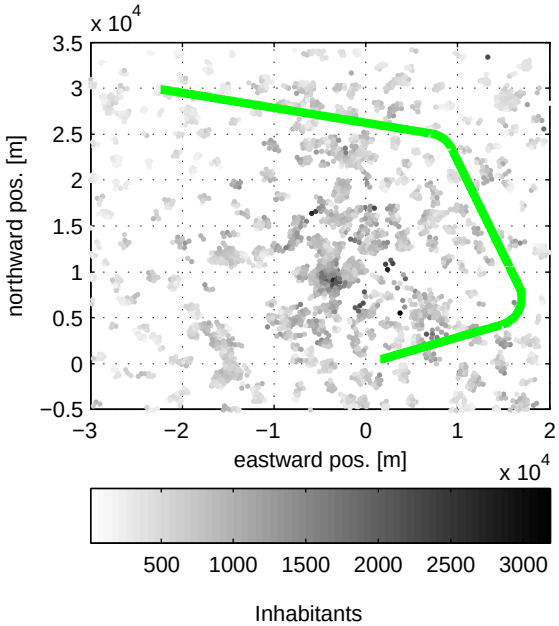

Fig. 2 Scenario layout

For comparison, three different optimizations are performed, which vary in the weighting for the upper level cost function as given in Table 1. In the optimization, the initial point (the runway threshold) and the final point have been fixed.

	Noise	Flight Time
Case 1	1	0
Case 2	.5	.5
Case 3	.2	.8
Case 4	0	1

Table 1 Upper level cost function weights

The horizontal flight path consist of six Track-To-Fix and five Radius-To-Fix segments, thus allowing a considerable curved trajectory. Table 2 summarizes the results for the different optimization cases in terms of number of awakenings, flight time and fuel consumption. The objective of the lower level problem was to minimize fuel consumption in all cases. Fig. 3 shows the resulting horizontal trajectory for all four cases. As the numerical results suggest, the trajectories for Case 1 and Case 2 are nearly the same.

	n_{awak} [-]	t_f [s]	$m_{fuel}[kg]$
Case 1	9180	855.6	710.3
Case 2	9182	852.7	708.5
Case 3	9506	722.5	634.2
Case 4	12820	527.4	527.9

Table 2 Optimization results

Compared to the minimum time case (Case 4) the minimum noise case (Case 1) reduces the number of awakenings by nearly 30%. However, fuel consumption and flight time are significantly increased. As airlines are in a fierce competition, it becomes clear that the weighting has to be chosen carefully.

6 Conclusion

Within this paper a bi-level optimal control problem and its solution has been described, that allows the computation of noise minimal departure procedures. By optimizing the fuel consumption in the lower level problem, it is possible to generate more realistic departure profiles than in the approaches available in the literature. Even though the parameterization of the horizontal flight path used within the optimization resembles RNAV (RNP) trajectories, the results have to be manually adapted for practicability. The stated bi-level optimal control problem has been successfully solved with an optimization framework developed by the authors. For future research it is foreseen to include further parameters into the upper level problem like minimum climb rates, etc. to have more influence on the departure procedure. Furthermore, it is planned to optimize a full scenario with multiple approach and departure trajectories simultaneously. This way, it is possible to take interdependencies between approach and departure procedures into account as in practice the departing traffic stream is normally routed below the arriving one.

References

[1] Visser, H. G. and Wijnen, R. A. A., Optimization of noise abatement departure procedures, *Journal of Aircraft*, Vol. 38, No. 4, pp. 620-627, 2001

[2] Prats, X., Puig, V. and Quevedo, J., Equitable aircraft noise-abatement departure procedures, *Journal of Guidance, Control, and Dynamics*, Vol. 34, No. 1, pp. 192-203, 2011

[3] Fisch, F., et al., Noise-minimal approach trajectories in mountainous areas, *AIAA Guidance, Navigation, and Control Conference*, Minneapolis, Minnesota, 2012

[4] Richter, M. and Holzapfel, F., Robust noise optimal approaches, *AIAA Guidance, Navigation, and Control Conference*, Boston, Massachusetts, 2013

[5] Fisch,F., Lenz, J., Holzapfel, F., Sachs, G., Solution of bilevel optimal control problems to increase fairness in air races, *Journal of Guidance, Control, and Dynamics*, Vol. 35, No. 4, pp. 1292-1298, 2012

[6] Betts, J., *Practical methods for optimal control and estimation using nonlinear programming*, SIAM, Philadelphia, 2010

[7] Büskens, C. and Maurer, H., SQP-methods for solving optimal control problems with control and state constraints: adjoint variables, sensi-

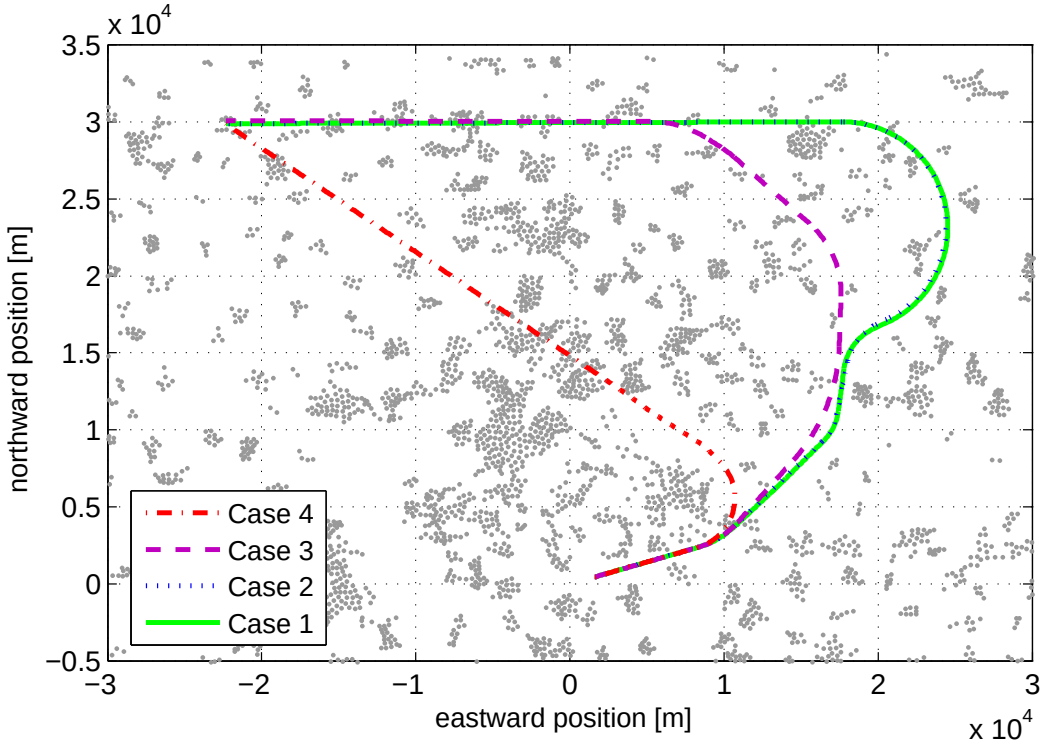

Fig. 3 Optimized horizontal trajectories

tivity analysis and real-time control, *Journal of Computational and Applied Mathematics*, Vol. 120, pp. 85-108, 2000

[8] ICAO *DOC 8168 Procedures for Air Navigation Serices*, Fifth Edition, 2006

[9] Wächter, A. and Biegler, L. T., On the implementation of a primal-dual interior point filter line search algorithm for large-scale nonlinear programming *Mathematical Programming* 106(1), pp.25-57, 2006

[10] Office of Environment and Energy, *Integrated Noise Model, Version 7.0, Technical Manual*, 2008

[11] Gallego, F., A population density grid of the European Union, *Population and Environment*, Vol. 31, No. 6, pp. 460-473, 2010

[12] Figlar, B., *The potential of noise abatement procedures to sustain traffic growth within airport noise constraints*, Dr. Hut Verlag, 2013

[13] Wassels, D. and Büskens, C., Modeling and optimization in space engineering, *Springer Optimization and its Applications*, Vol. 73, Springer Verlag, 2013

[14] Gill, P.E., Murray, W., Saunders, M.A.,*User's guide for SNOPT Version 7: Software for large-scale nonlinear programming*, University of California, Department of Mathematics, San Diego, CA, 2007

[15] *Effects of aviation noise on awakenings from sleep*, Federal Interagency Committee on Aviation Noise (FICAN), 1997

7 Contact Author Email Address

mailto:maximilian.richter@tum.de

Copyright Statement